International Journal of Fracture **65:** 261–276, 1994.

The stability of delamination growth in compressively loaded composite plates

G.A. KARDOMATEAS and A.A. PELEGRI
School of Aerospace Engineering, Georgia Institute of Technology, Atlanta, Georgia 30332-0150, USA

Received 11 May 1993; accepted in revised form 6 January 1994

Abstract. The stability of growth of internal delaminations in composite plates subjected to compressive loading is investigated. Due to the compressive loading, these structures can undergo buckling of the delaminated layer and subsequently growth of the delamination. The study does not impose any restrictive assumptions regarding the delamination thickness and plate length (as opposed to the usual thin film assumptions). The growth characteristics of the delamination under monotonic compressive loading are obtained on the basis of a combined delamination buckling/postbuckling and fracture mechanics model. The postbuckling solution is derived through a perturbation procedure, which is based on an asymptotic expansion of the load and deformation quantities in terms of the distortion parameter of the delaminated layer, the latter being considered a compressive elastica. The closed form solutions for the energy release rate at the delamination tip versus applied compressive strain during the initial postbuckling phase are used to define the combinations of delamination length and applied strain that lead to unstable growth. This would practically cause either contained "jump" growth or complete (catastrophic) growth of the delamination. Estimates for the lower and upper bounds of the jump distance (unstable growth) are provided. Moreover, a study of the influence of the mode dependence of interface toughness on the conditions of initiation and extent of delamination growth is performed.

1. Introduction

Laminated composites have a high strength in the direction of the reinforcing fibers but are very sensitive to delamination-type defects. Indeed, the manufacture of composites requires involved procedures which may potentially result in the existence of defects in the finished product [1]. Therefore, in these composite panels, local spalling or debonding may occur due to manufacturing imperfections or due to service loads which include impact, and vibrations excited by the propulsion systems.

Delamination buckling in plates under compression has received considerable attention and numerous contributions have addressed related issues in both one-dimensional [2–7] and two-dimensional treatments [8–10]. Moreover, the Griffith–Irwin concept has already been used in these works when the stable growth of thin delaminations in plane elements is investigated.

The growth characteristics of the delamination can be investigated once a post-buckling solution is available. Therefore, a combined fracture mechanics analysis and delamination post-buckling solution is needed. This subject makes for a non-traditional problem of fracture mechanics since the determination of the postbuckling deflections of a thin debonded layer when a plate element is subjected to cyclic compression is geometrically nonlinear and includes the explicit presence of additional parameters with the dimension of the length (e.g. the thickness of the separated layer or the plate length). To this extent, some fundamental features of the energy release rate characterization at the tip of delaminations have already been published. In fact, one particular result that is used within, namely the closed form expression for the energy release rate from the thin film model of Chai et al. [2], is directly extracted from that earlier article.

The criterion for the initiation of delamination propagation (fracture criterion) does not

follow from the equations of equilibrium and motion of continuum mechanics; it is rather an additional boundary condition in the solution of the problem of the limiting equilibrium for the delaminated body. This additional condition is postulated a-priori, and in this paper a mode-dependent condition will be examined in addition to the classical mode-independent critical energy release rate criterion.

After the body reaches the limiting equilibrium state, the delamination growth may be either stable or unstable. In a stable state, the delamination is stationary under constant external load and the delamination extension over a small distance requires a small increment of the applied external loading parameter. Conversely, in an unstable equilibrium state, the delamination begins to move after the load reaches the critical value determined from the fracture criterion and may even propagate under constant load. Naturally, dynamic effects are involved in the latter case. As far as the prevention of integrity loss is concerned, it is important to know the kind of equilibrium to which the limiting state belongs. If the limiting equilibrium state is stable, there is no danger of immediate uncontrollable propagation of the delamination.

A delaminated layer loses stability at a critical point, the determination of which is first needed. In a fundamental paper, Chai, Babcock and Knauss [2] presented a one-dimensional model by assuming essentially a delamination in an infinitely thick plate. In this model (which has also been called 'thin film' model), the unbuckled (base) plate is assumed to be subject to a uniform compressive strain. Calculation of the strain energy of the buckled layer, the one for the layer prior to loss of stability and the work performed by the applied load are used in the calculation of the energy release rate, i.e. the energy released when the delamination grows by a unit of length. Energy release rate and delamination length curves for a constant applied strain can reveal the regions where the delamination growth is stable or unstable.

In the general case, the finite plate length and thickness is expected to influence the bifurcation point and post-critical behavior of the delamination and subsequently its growth characteristics. An additional influence may also arise from the end fixity conditions of the base plate. To this extent, Simitses et al. [7] studied the critical load for a delamination of arbitrary thickness and size in a finite plate; their results showed a range of critical load vs. thin film load ratios, depending on delamination and base plate dimensions, as well as base plate end fixity (simply-supported vs. clamped).

In a recent paper, Kardomateas [11] studied the initial postbuckling behavior of general delaminated composites (i.e. with no restrictive assumptions on the delamination dimensions) by using a perturbation procedure based on an asymptotic expansion of the load and deformation quantities in terms of the distortion parameter of the delaminated layer, the latter being considered a compressive elastica. The analysis lead to closed form solutions for the load versus applied compressive displacement and the near tip resultant moments and forces. This postbuckling solution is used in this paper to study the stability of growth of internal delaminations as well as some other important characteristics of the growth process. For this purpose, the bimaterial interface crack solutions for the energy release rate and the mode mixity in terms of the resultant moments and forces, as derived by Suo and Hutchinson [12] will be employed. A primary objective is to define the combinations of delamination length and applied strain that lead to unstable growth; this would practically cause a 'jump' growth (mostly contained) of the delamination. Results that reveal under what conditions growth becomes unstable will be presented for a variety of delamination locations through the thickness and will be compared with the thin film model theory. Another objective of this paper is to include the mode dependence of interface toughness and study its qualitative influence on the conditions of initiation and extent of delamination growth.

2. Stable and unstable delamination growth

The stability of delamination growth will be studied next. In order to better illustrate the combined post-critical and fracture mechanics procedure for obtaining the conditions for unstable or stable growth, the simple relations from the thin film model will be used. For simplicity reasons, the properties of the material are assumed homogeneous, linearly elastic and isotropic with modulus of elasticity E and Poisson's ratio ν (orthotropic properties can be accounted for by using $\nu_{12}\nu_{21}$ instead of ν^2 and E the modulus of elasticity along the $x \equiv 1$ axis).

For a delamination of thickness h and half-length ℓ, the thin film model of Chai et al. [2] predicts an energy release rate

$$G(\varepsilon_0, \ell) = \tfrac{1}{2}Eh(1-\nu^2)(\varepsilon_0^2 + 2\varepsilon_0\varepsilon_{cr} - 3\varepsilon_{cr}^2), \tag{1}$$

where

$$\varepsilon_{cr} = \frac{\pi^2 h^2}{12(1-\nu^2)\ell^2}, \tag{2}$$

is the Euler's critical strain for the delaminated layer (treated as a column with built-in ends) and ε_0 is the applied strain. A Griffith-type fracture criterion is employed, and it is assumed that whether further delamination occurs depends on the magnitude of the fracture energy, defined as the energy required to produce a unit of new delamination. Thus, delamination growth occurs when

$$G(\varepsilon_0, \ell) = \Gamma_0 = \text{const.} \tag{3}$$

Let us assume that the delamination growth is governed by the external 'loading' quantity $\varepsilon_0(\ell)$ (i.e. the applied strain). In a stable state, the delamination is stationary under constant ε_0 and the delamination extension over a small area (or through a small distance) also requires a small increment of the applied strain ε_0. Consequently, in the expression between the applied strain and the delamination length $\varepsilon_0 = \varepsilon_0(\ell)$ found from the fracture criterion $G(\varepsilon_0, \ell) = \Gamma_0$, for a stable delamination

$$\left(\frac{d\varepsilon_0}{d\ell}\right)_G > 0. \tag{4a}$$

An inequality expression for the energy release rate for stable growth can also be found as follows. While the delamination growth proceeds, $G(\varepsilon_0, \ell)$ satisfies (3), and thus

$$\frac{dG}{d\ell} = \left(\frac{\partial G}{\partial \varepsilon_0}\right)_\ell \frac{d\varepsilon_0}{d\ell} + \left(\frac{\partial G}{\partial \ell}\right)_{\varepsilon_0} = 0. \tag{4b}$$

Since it can generally be assumed [see e.g. (1)] that $(\partial G/\partial \varepsilon_0)_\ell > 0$, it follows that for stable growth

$$\left(\frac{\partial G}{\partial \ell}\right)_{\varepsilon_0} < 0. \tag{4c}$$

The stable and unstable equilibrium branches corresponding to this condition are illustrated in Fig. 1.

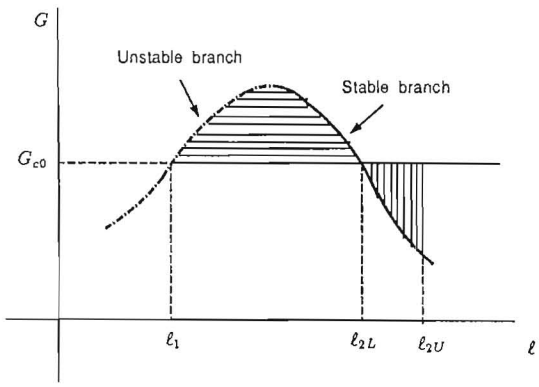

Fig. 1. Equilibrium branches for stable and unstable delamination growth (for a given applied compressive strain), illustrating the contained 'jump' growth of a delamination loaded on the unstable branch.

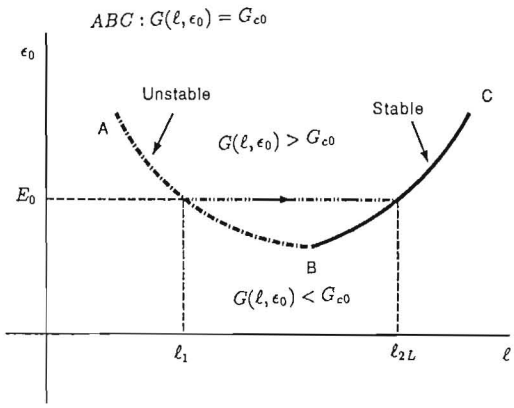

Fig. 2 Equilibrium branches for stable and unstable delamination growth for a given critical energy release rate.

In an unstable equilibrium state, the delamination may propagate under constant applied strain ε_0 (Fig. 2), and in this case the following inequality expressions define the range of unstable equilibrium states

$$\left(\frac{d\varepsilon_0}{d\ell}\right)_G \leqslant 0; \quad \text{or} \quad \left(\frac{\partial G}{\partial \ell}\right)_{\varepsilon_0} \geqslant 0. \tag{5}$$

Now, applying $G(\varepsilon_0, \ell) = \Gamma_0$ in (1) and solving for ε_0, we find

$$\varepsilon_0 = -\varepsilon_{cr} + \sqrt{4\varepsilon_{cr}^2 + \frac{2\Gamma_0}{Eh(1-\nu^2)}}. \tag{6}$$

The transition from stable to unstable growth occurs when

$$\frac{d\varepsilon_0}{d\ell} = (-\varepsilon_0 + 3\varepsilon_{cr})\frac{-2\pi^2 h^2}{3\ell^3} = 0, \tag{7a}$$

which gives

$$\varepsilon_0 = 3\varepsilon_{cr}. \tag{7c}$$

Therefore, we have stable crack growth if

$$\varepsilon_0 > 3\varepsilon_{cr}, \tag{8a}$$

and unstable growth if

$$\varepsilon_0 < 3\varepsilon_{cr}. \tag{8b}$$

The same conclusion is reached if we use the criterion in terms of the energy release rate from (5)

$$\left(\frac{dG}{d\ell}\right)_{\varepsilon_0} = Eh(1-\nu^2)(\varepsilon_0 - 3\varepsilon_{cr})\frac{d\varepsilon_{cr}}{d\ell} = 0. \tag{8c}$$

Let us assume that at length ℓ_1, the delamination falls on an unstable branch (Fig. 1). Then, growth will take place to a new delamination size ℓ_2. The lower bound of the new delamination size ℓ_{2L} corresponds to the equation $G(\varepsilon_0, \ell_{2L}) = \Gamma_0$, i.e. it is determined from the position of the stable branch, since for any size smaller than that $G > \Gamma_0$. The upper bound to the new delamination size ℓ_{2U} can be found from an energy balance as the delamination increases from ℓ_1 to ℓ_2. Indeed, the energy that must be expended for an infinitesimal growth (fracture energy) is $\Gamma_0 d\ell$, whereas the energy released and attributed to the fracture process is $G(\varepsilon_0, \ell)d\ell - dT$, where dT is the (undetermined) kinetic energy. Therefore, the lowest possible value of the difference $[G(\varepsilon_0, \ell) - \Gamma_0]d\ell$ is zero, corresponding to zero kinetic energy $dT = 0$. Hence, the upper bound is found from

$$\int_{\ell_1}^{\ell_{2U}} G(\varepsilon_0, \ell)d\ell = \Gamma_0(\ell_{2U} - \ell_1). \tag{9}$$

In this case of unstable growth, the difference $[G(\varepsilon_0, \ell) - \Gamma_0]d\ell$ represents the kinetic energy dT, assumed to be zero for quasistatic growth. Notice that $G(\varepsilon_0, \ell)d\ell$ represents the total energy released in the process due to the work done by the external forces W and the change in the elastic strain energy dU i.e. $G(\varepsilon_0, \ell)d\ell = W - dU$.

This relationship is shown schematically in Fig. 1; the areas indicated by different shadings are of equal size.

For the thin film model, a nonlinear equation for the upper bound of the unstable delamination growth can be derived (this has also been discussed by Bolotin [4]). Indeed, using (1) for the energy release rate, we find

$$\int G(\varepsilon_0, \ell)d\ell = \tfrac{1}{2}Eh(1-\nu^2)[\varepsilon_0 - \varepsilon_{cr}(\ell)]^2\ell, \tag{10a}$$

therefore, using (9), the upper bound, ℓ_{2U}, is found from the nonlinear equation

$$[\varepsilon_0 - \varepsilon_{cr}(\ell_{2U})]^2\ell_{2U} - [\varepsilon_0 - \varepsilon_{cr}(\ell_1)]^2\ell_1 = \frac{2\Gamma_0}{Eh(1-\nu^2)}(\ell_{2U} - \ell_1). \tag{10b}$$

3. Growth characteristics for a delamination of arbitrary thickness

A closed form solution for the initial postbuckling solution in the general case (arbitrary delamination thickness or plate length) has recently been derived by Kardomateas [11]. The latter will be briefly described first and then it will be used to determine the stable and unstable growth conditions of an arbitrary delamination.

Referring to Fig. 3, consider a plate of half-length L (and unit width) with a through-the-width delamination of half-length ℓ, symmetrically located. The delamination is at an arbitrary position through the thickness T. Over the delaminated region, the laminate consists of the part above the delamination, of thickness h referred to as the 'delaminated' part, and the part below the delamination, of thickness $H = T - h$, referred to as the 'substrate' part. The remaining, intact laminate, of thickness T and length $b = L - \ell$, is referred to as the 'base' plate. Accordingly, the subscript $i = d, s, b$ refers to the delaminated part, the substrate or the base plate, respectively.

The solution in [11] is based on considering the buckled configuration of the delaminated layer as part of an inflectional elastica with end amplitude Φ_d and distortion parameter ε. At

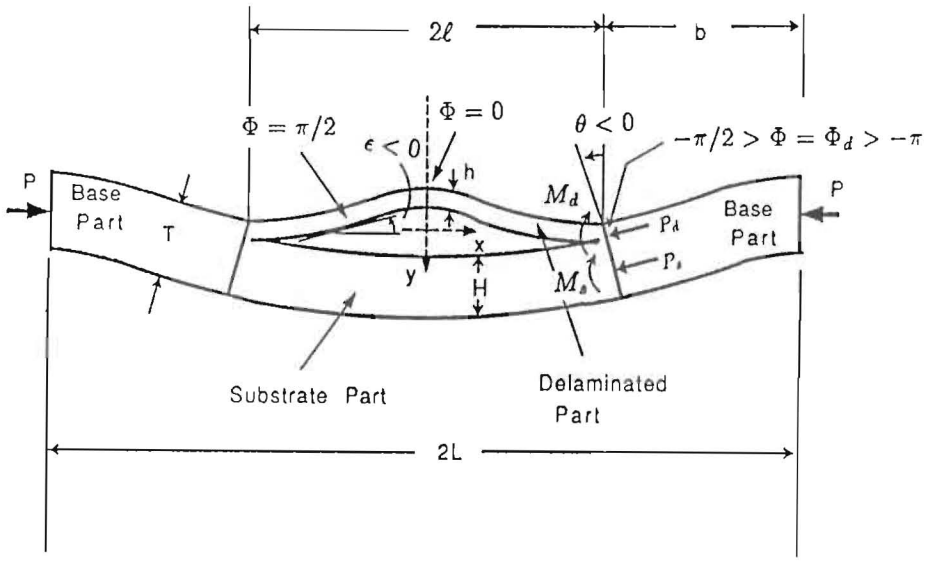

Fig. 3. A compressively loaded one-dimensional delamination configuration in the post-critical state.

the critical state, the end amplitude is Φ_d^0. Suppose that in the slightly buckled configuration Φ_d can be expanded in the form

$$\Phi_d = \Phi_d^0 + \phi_d^{(1)}\varepsilon + \phi_d^{(2)}\varepsilon^2 + O(\varepsilon^3). \tag{11}$$

Then the end rotation at the common section θ is given by expanding the relevant expression [13] in Taylor series in terms of ε (notice that at the critical state $\theta^0 = 0$)

$$\begin{aligned}\theta &= (\sin\Phi_d)\varepsilon - \tfrac{1}{24}(\sin\Phi_d\cos^2\Phi_d)\varepsilon^3 + \cdots = (\sin\Phi_d^0)\varepsilon + (\cos\Phi_d^0)\phi_d^{(1)}\varepsilon^2 + \\ &+ \left[(\cos\Phi_d^0)\phi_d^{(2)} - (\sin\Phi_d^0)\frac{\phi_d^{(1)2}}{2} - \tfrac{1}{24}\sin\Phi_d^0\cos^2\Phi_d^0\right]\varepsilon^3 + \cdots = \\ &= \theta^{(1)}\varepsilon + \theta^{(2)}\varepsilon^2 + \theta^{(3)}\varepsilon^3 + O(\varepsilon^4).\end{aligned} \tag{12}$$

Due to the continuity condition θ is the same for both the delaminated and substrate parts as well as the base plate.

The asymptotic expansion for the end moment M_d is similarly found by substituting (1) into the relevant expression [13] and subsequently expanding in Taylor series (again $M_d^0 = 0$)

$$\begin{aligned}\frac{\ell M_d}{D_d} &= (\Phi_d\cos\Phi_d)\varepsilon + \frac{\Phi_d}{16}\left(\frac{1}{3} - \frac{\sin 2\Phi_d}{2\Phi_d}\right)(\cos\Phi_d)\varepsilon^3 + \cdots = \\ &= \frac{\ell}{D_d}(M_d^{(1)}\varepsilon + M_d^{(2)}\varepsilon^2 + M_d^{(3)}\varepsilon^3) + O(\varepsilon^4),\end{aligned} \tag{13a}$$

where $D_d = Eh^3/[12(1-\nu^2)]$, is the bending stiffness, and

$$\frac{\ell M_d^{(1)}}{D_d} = \Phi_d^0\cos\Phi_d^0; \quad \frac{\ell M_d^{(2)}}{D_d} = (\cos\Phi_d^0 - \Phi_d^0\sin\Phi_d^0)\phi_d^{(1)}, \tag{13b}$$

$$\frac{\ell M_d^{(3)}}{D_d} = (\cos\Phi_d^0 - \Phi_d^0 \sin\Phi_d^0)\phi_d^{(2)} - \left(\sin\Phi_d^0 + \frac{\Phi_d^0}{2}\cos\Phi_d^0\right)\phi_d^{(1)2} + \\ + \frac{\Phi_d^0}{16}\left(\frac{1}{3} - \frac{\sin 2\Phi_d^0}{2\Phi_d^0}\right)(\cos\Phi_d^0). \tag{13c}$$

Likewise, the axial force P_d and the flexural contraction f_d can be found in an asymptotic expansion form.

Although the substrate part and the base plate undergo moderate bending with no inflection point, we may also use the elastica theory to describe their (nonlinear) deformation; in this case the inflection points are outside the actual elastic curve. For the substrate part, we have to expand not only the amplitude Φ_s, but also the distortion parameter α_s in a perturbation series with respect to the distortion parameter of the delaminated layer ε

$$\Phi_s = \Phi_s^0 + \phi_s^{(1)}\varepsilon + \phi_s^{(2)}\epsilon^2 + O(\varepsilon^3), \tag{14a}$$

$$\alpha_s = \alpha_s^{(1)}\varepsilon + \alpha_s^{(2)}\varepsilon^2 + \alpha_s^{(3)}\varepsilon^3 + O(\varepsilon^4). \tag{14b}$$

The base plate is assumed to be simply supported, so at the simply-supported end, the amplitude $\Phi = -\pi/2$, and at the common section $\Phi = \Phi_b$. The amplitude at the common section and the distortion parameter of the base plate are now expanded in terms of the distortion parameter of the delaminated part ε

$$\Phi_b = \Phi_b^0 + \phi_b^{(1)}\varepsilon + \phi_b^{(2)}\epsilon^2 + O(\varepsilon^3), \tag{15a}$$

$$\alpha_b = \alpha_b^{(1)}\varepsilon + \alpha_b^{(2)}\varepsilon^2 + \alpha_b^{(3)}\epsilon^3 + O(\varepsilon^4). \tag{15b}$$

The end rotation at the common section θ, the end moments M_s, M_b, the axial forces, P_s and P and the flexural contractions f_s and f_b can be found by expanding again in Taylor series in terms of ε.

Having obtained the asymptotic expressions for the force and deformation quantities, the equilibrium and compatibility requirements that ultimately define the non-linear post-critical path are the force and moment equilibrium at the common section and a condition that involves the compatible shortening of the delaminated and substrate parts. These conditions are imposed for the first order, second and third order terms separately and lead to:

(a) one nonlinear equation for the zero order terms, which defines the critical point (characteristic equation) and

(b) two linear algebraic equations for $\phi_d^{(1)}$ and $\phi_s^{(1)}$ that determine the first order forces and two linear algebraic equations for $\phi_d^{(2)}$ and $\phi_s^{(2)}$ that define the second order forces [11].

The initial postbuckling solution that has just been briefly described is used now in conjunction with the interface crack solutions summarized by Hutchinson and Suo [14]. For a general bimaterial interface crack, these solutions depend on the Dundurs [15] parameters, $\tilde{\alpha}$, $\tilde{\beta}$ and the bimaterial constant $\tilde{\varepsilon}$. For the homogeneous system under consideration, $\tilde{\alpha} = \tilde{\beta} = \tilde{\varepsilon} = 0$. Therefore these formulas will be presented with the homogeneous material assumption taken into consideration.

For the plane-strain interface crack shown in Fig. 3, the energy release rate, G, is

$$G = \frac{1-\nu}{4\mu}\left[\frac{P^{*2}}{Ah} + \frac{M^{*2}}{Ih^3} + 2\frac{P^*M^*}{\sqrt{AI}h^2}\sin\gamma\right]. \tag{16}$$

where μ is the shear modulus. In terms of

$$\eta = h/H; \quad C_1 = \frac{h}{T}; \quad C_2 = \frac{6h^2H}{T^3}; \quad C_3 = \frac{h^3}{T^3}, \tag{17}$$

P^* and M^* are linear combinations of the loads from the previous postbuckling solution

$$P^* = P_d - C_1P - C_2\frac{M_b}{h}, \tag{18a}$$

$$M^* = M_d - C_3M_b. \tag{18b}$$

Moreover, A and I are positive dimensionless numbers and the angle γ is restricted such that $\gamma \leqslant \pi/2$. These quantities are given by

$$A = \frac{1}{1+4\eta+6\eta^2+3\eta^3}; \quad I = \frac{1}{12(1+\eta^3)}; \quad \sin\gamma = 6\eta^2(1+\eta)\sqrt{AI}. \tag{19}$$

The preceding formula does not separate the opening and shearing components. Instead, the following two expressions give the mode I and mode II stress intensity factors:

$$K_{\mathrm{I}} = \frac{1}{\sqrt{2}}\left[\frac{P^*}{\sqrt{Ah}}\cos\omega + \frac{M^*}{\sqrt{Ih^3}}\sin(\omega+\gamma)\right], \tag{20a}$$

$$K_{\mathrm{II}} = \frac{1}{\sqrt{2}}\left[\frac{P^*}{\sqrt{Ah}}\sin\omega - \frac{M^*}{\sqrt{Ih^3}}\cos(\omega+\gamma)\right]. \tag{20b}$$

Accurate determination of ω, which depends only on η (for a fixed set of Dundurs constants $\tilde{\alpha}$, $\tilde{\beta}$), requires the numerical solution of an integral equation and has been reported in Suo and Hutchinson [12]. The extracted ω, however, varies slowly with η in the entire range $0 \leqslant \eta \leqslant 1$, in accordance with the approximate formula [14]

$$\omega = 52.1^0 - 3^0\eta. \tag{21}$$

The mode mixity is defined by

$$\psi = \tan^{-1}(K_{\mathrm{II}}/K_{\mathrm{I}}) = \tan^{-1}\left[\frac{\tilde{\lambda}\sin\omega - \cos(\omega+\gamma)}{\tilde{\lambda}\cos\omega + \sin(\omega+\gamma)}\right], \tag{22a}$$

where $\tilde{\lambda}$ measures the loading combination as

$$\tilde{\lambda} = \sqrt{\frac{I}{A}}\frac{P^*h}{M^*}. \tag{22b}$$

Substituting the asymptotic expressions for the forces and moments from the postbuckling solution already presented, gives

$$P^* = \varepsilon P^{*(1)} + \varepsilon^2 P^{*(2)} + \cdots, \quad M^* = \varepsilon M^{*(1)} + \varepsilon^2 M^{*(2)} + \cdots, \tag{23a}$$

where the first and second order terms (i.e. $k = 1, 2$) are (notice that the zero order quantities in the expression for P^* cancel out)

$$P^{*(k)} = \frac{H}{T}P_d^{(k)} - \frac{h}{T}P_s^{(k)} - \frac{6hH}{T^3}M_b^{(k)}, \tag{23b}$$

$$M^{*(k)} = M_d^{(k)} - \frac{h^3}{T^3}M_b^{(k)}. \tag{23c}$$

In the previous relations, the first and second order forces and moments $P_d^{(k)}$, $P_s^{(k)}$, $M_d^{(k)}$, $M_b^{(k)}$, $k = 1, 2$ have already been found from the initial postbuckling solution of [11], which was also briefly described in this section.

Now the energy release rate and the mode I and II stress intensity factors can be written in the form:

$$G = \varepsilon^2 G^{(2)} + \varepsilon^3 G^{(3)} + \cdots, \tag{24a}$$

$$K_{\mathrm{I,II}} = \varepsilon K_{\mathrm{I,II}}^{(1)} + \varepsilon^2 K_{\mathrm{I,II}}^{(2)} + \cdots, \tag{24b}$$

where $K_{\mathrm{I,II}}^{(1)}$, $K_{\mathrm{I,II}}^{(2)}$ are found by substituting in (20) the first or second order forces and moments, respectively, $G^{(2)}$ is found from (16) by substituting directly the first order forces and moments, and

$$G^{(3)} = \frac{1-\nu}{2\mu}\left[\frac{P^{*(1)}P^{*(2)}}{Ah} + \frac{M^{*(1)}M^{*(2)}}{Ih^3} + \frac{\sin\gamma}{\sqrt{AI}h^2}(P^{*(1)}M^{*(2)} + P^{*(2)}M^{*(1)})\right]. \tag{24c}$$

The other quantity that is needed to assess the stability of delamination growth is the applied strain ε_0 which is the external 'loading' quantity. This is given as follows

$$\varepsilon_0 = \varepsilon_0^{(0)} + \varepsilon_0^{(1)}\varepsilon + \varepsilon_0^{(2)}\varepsilon^2, \tag{25a}$$

where

$$\varepsilon_0^{(0)} = \frac{P^0}{ET}; \quad \varepsilon_0^{(1)}L = \frac{P^{(1)}b}{ET} + \frac{P_d^{(1)}\ell}{Eh} + \frac{H}{2}\theta^{(1)}, \tag{25b}$$

$$\varepsilon_0^{(2)}L = \frac{f_d^{(2)}}{2} + \frac{P_d^{(2)}\ell}{Eh} + f_b^{(2)} + \frac{P^{(2)}b}{ET} + \frac{H}{2}\theta^{(2)}. \tag{25c}$$

The construction of $G - \ell$ or $E_0 - \ell$ curves as in Figs. 2, 3 will be described next. Let us discuss first the family curves of applied strain versus delamination length, $\varepsilon_0(\ell)$ for different values of G (e.g. Fig. 2). This is done as follows: For a specified $G = \Gamma_0$, the corresponding ε is determined from the minimum (negative) root of the equation

$$\Gamma_0 = G^{(2)}(\ell)\varepsilon^2 + G^{(3)}(\ell)\varepsilon^3. \tag{26a}$$

The corresponding applied strain is

$$\varepsilon_0(\ell) = \varepsilon_0^{(0)}(\ell) + \varepsilon_0^{(1)}(\ell)\varepsilon + \varepsilon_0^{(2)}(\ell)\varepsilon^2. \tag{26b}$$

In a similar fashion, the family curves of the energy release rate as a function of delamination length $G(\ell)$ for different values of applied strain ε_0 (e.g. Fig. 1) are plotted as follows: For a specified $\varepsilon_0 = E_0$, the corresponding ε is determined from the minimum (negative) root of the equation

$$E_0 = \varepsilon_0^{(0)}(\ell) + \varepsilon_0^{(1)}(\ell)\varepsilon + \varepsilon_0^{(2)}(\ell)\varepsilon^2. \tag{27a}$$

Then, the corresponding energy release rate is

$$G(\ell) = G^{(2)}(\ell)\varepsilon^2 + G^{(3)}(\ell)\varepsilon^3. \tag{27b}$$

According to (5), the delamination growth is stable if the $\varepsilon_0 - \ell$ curve has a positive slope or the $G - \ell$ curve a negative slope, and it is unstable otherwise.

4. Effect of mode-dependence on the fracture toughness

The previous analysis was based on assuming a mode-independent critical energy release rate; this would mean, for example, $\Gamma_0 = G_I^c$. During the initial postbuckling phase, the mode mixity changes with applied strain, and depends on the relative delamination thickness h/T. For example, the study in [11] has shown that a higher mode I component is present with delaminations further away from the surface.

Based on these observations, let us now assume that the toughness Γ_0 depends on the mode mixity ψ, and in fact $\Gamma_0(\psi)$ increases with increasing $|\ \psi\ |$ (increasing mode II component). A simple, one parameter family of mixed mode adjusted fracture criteria can be described by [14]

$$\Gamma_0(\psi) = G_I^c[1 + (\lambda - 1)\sin^2\psi]^{-1}. \tag{28}$$

The parameter λ adjusts the influence of the mode II contribution in the criterion. The limit $\lambda = 1$ is the case of the classical mode-independent toughness, i.e. $\Gamma_0 = G_I^c$ for all mode combinations (note that G_I^c is the pure mode I toughness). Other phenomenological criteria have been proposed to characterize mixed mode toughness data for interlaminar fracture such as in [16]. One other alternative phenomenological criterion is:

$$\Gamma_0(\psi) = G_I^c[1 + (1 - \lambda)\tan^2\psi]. \tag{29}$$

According to (28), the fracture toughness levels off as $\psi \to 90°$ (mode II), whereas (29) models the toughness as unbounded as $\psi \to 90°$ for all $\lambda < 1$. As was discussed in [14], while this feature should not be taken literally, it did emerge in the simple model of mixed mode interface toughness due to asperity contact of Evans and Hutchinson [17].

Returning now to the delamination growth during the initial postbuckling phase, to see the effects of mode-dependent toughness on the growth characteristics, curves of $G/\Gamma_0(\psi)$ versus delamination length ℓ at various levels of applied strain ε_0 are constructed. Then $G/\Gamma_0(\psi)$ can be regarded as a mode-adjusted crack driving force in the sense that the criterion for crack advance is $G/\Gamma_0(\psi) = G_I^c$. Two values of λ, 0.15 and 0.30 are used.

For the thin film model, the mode mixity is

$$\tan\psi = \frac{4\cos\omega + \sqrt{3}\xi\sin\omega}{-4\sin\omega + \sqrt{3}\xi\cos\omega}, \tag{30a}$$

where

$$\xi = \left[\frac{4}{3}\left(\frac{\varepsilon_0}{\varepsilon_{cr}} - 1\right)\right]^{1/2}; \quad \omega = 52.1^0. \tag{30b}$$

Therefore, if we define

$$\tilde{G} = G/\Gamma_0(\psi) = \tilde{G}(\varepsilon_0, \varepsilon_{cr}, \psi), \tag{31}$$

since

$$\psi = \psi(\varepsilon_0, \varepsilon_{cr}),$$

we can write

$$\left(\frac{d\tilde{G}}{d\ell}\right)_{\varepsilon_0} = \left(\frac{\partial\tilde{G}}{\partial\varepsilon_{cr}} + \frac{\partial\tilde{G}}{\partial\psi}\frac{\partial\psi}{\partial\varepsilon_{cr}}\right)\frac{d\varepsilon_{cr}}{d\ell}.$$

Substituting the definitions of ψ from (30) and $\Gamma_0(\psi)$ from (28) we obtain the unstable-to-stable transition point

$$(\varepsilon_0 - 3\varepsilon_{cr}) + \frac{(\varepsilon_0^2 + 2\varepsilon_0\varepsilon_{cr} - 3\varepsilon_{cr}^2)}{[1 + (\lambda - 1)\sin^2\psi]}(\lambda - 1)\frac{1}{(3\xi^2 + 16)}\frac{4}{\sqrt{3}\xi}\frac{\varepsilon_0}{\varepsilon_{cr}^2}\sin 2\psi = 0. \tag{32}$$

Likewise, for the fracture condition (29), the unstable-to-stable transition point in the thin film model is defined from

$$(\varepsilon_0 - 3\varepsilon_{cr}) + \frac{(\varepsilon_0^2 + 2\varepsilon_0\varepsilon_{cr} - 3\varepsilon_{cr}^2)}{[1 + (\lambda - 1)\tan^2\psi]}(\lambda - 1)\frac{1}{(3\xi^2 + 16)}\frac{8}{\sqrt{3}\xi}\frac{\varepsilon_0}{\varepsilon_{cr}^2}\frac{\tan\psi}{\cos^2\psi} = 0. \tag{33}$$

For the general case of arbitrary delamination and plate dimensions, the post-buckling solution by Kardomateas [11] can be used to derive the mode mixity ψ in a closed form expression. In this case, the family curves of the energy release rate, $\tilde{G} = G/\Gamma_0(\psi)$ as a function of delamination length for different values of applied strain ε_0 are plotted. For a specified $\varepsilon_0 = \varepsilon_0^P$, the corresponding ε is again determined from the minimum (negative) root of (27a) and the corresponding energy release rate, G is again found from (27b) whereas the mode mixity ψ is found from

$$\psi = \tan^{-1}\frac{\varepsilon K_{II}^{(1)} + \varepsilon^2 K_{II}^{(2)}}{\varepsilon K_I^{(1)} + \varepsilon^2 K_I^{(2)}}. \tag{34}$$

5. Discussion of results

For an illustration of the results from the previous analysis for a delamination of arbitrary thickness, consider a delaminated plate with $E = 70\,\text{GPa}$ and $\nu = 0.3$ and half-length $L = 60\,\text{mm}$. These dimensions correspond to our specimen dimensions (a width of 10 mm has also been considered and is appropriately accounted for in the results). A delamination thickness of $h = 0.4\,\text{mm}$ is assumed whereas the delamination length is varying.

To ensure the same thin film model solution in the results that follow (for a chosen delamination length), we keep the delamination thickness constant and change only the plate thickness; this would give a varying ratio h/T.

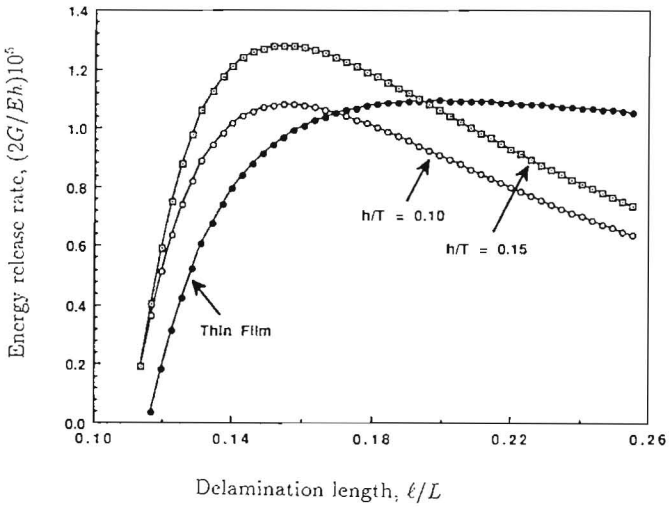

Fig. 4. The energy release rate as a function of the delamination length (for a specific applied strain $E_0 = 3.0 \times 10^{-3}$). In each curve, the zero slope or peak value is the unstable-to-stable transition point.

Figure 4 shows the energy release rate $(2G/Eh)10^5$, as a function of the delamination length ℓ/L, for a specified applied strain $E_0 = 3.0 \times 10^{-3}$ and two cases: $h/T = 0.10$ and $h/T = 0.15$, in comparison with the thin film solution. It is seen that the unstable-to-stable transition point (zero slope or peak value) is shifted to the left with respect to the corresponding point in the thin film solution. The ratio $E_0/\varepsilon_{cr}(\ell_{tr}) = E_0 12\ell_{tr}^2/\pi^2 h^2$, where ℓ_{tr} is the delamination length at this transition point, is always three for the limiting thin film solution as has already been discussed. It is found that this ratio in the general case is less than three; in this particular example, for the other two cases this ratio is close to two. This would suggest that the delamination growth is less likely to be unstable since the range of delamination lengths for unstable growth is reduced.

Another observation is that beyond ℓ_{tr} (peak point) the curves for $h/T = 0.10$, 0.15 are steeper than the thin film model approximation (steeper for the higher h/T ratio); therefore, the jump distance (unstable growth) is smaller than the one predicted by the thin film model (see also Fig. 1). Assuming a critical energy release rate $\Gamma_0 = 120\,\text{N/m}$, or $(2\Gamma_0/Eh)10^5 = 0.857$, the $G - \ell$ curve for $E_0 = 2.8 \times 10^{-3}$, $h/T = 0.10$, would predict unstable growth at $\ell/L = 0.143$. A lower bound on the jump distance (delamination growth) ℓ_j is found from the stable branch of Fig. 4: $\ell_{jL}/L = 0.047$; applying (9) gives the upper bound at $\ell_{jU}/L = 0.080$. In comparison, the thin film model would predict unstable growth at $\ell/L = 0.163$ and a very large jump (indeed the lower bound, i.e. the end point on the stable branch would be beyond the scale of delamination lengths shown in Fig. 4).

The stability of delamination growth can be also assessed from the plot of the applied strain versus delamination length for a chosen value of the energy release rate. This is illustrated in Fig. 5 which shows E_0 as a function of the delamination length ℓ/L, for the specified value of the energy release rate, $(2G/Eh)10^5 = 1.3$. The two cases, $h/T = 0.10$ and $h/T = 0.15$, in comparison with the thin film solution are again being shown (see also Fig. 2). Similar conclusions are drawn, i.e. the point of zero slope (lowest value in the $E_0 - \ell$ plot) which is the unstable-to-stable transition point is shifted to the left with respect to the corresponding one in the thin film solution and the ratio $E_0/\varepsilon_{cr}(\ell_{tr})$ (where ℓ_{tr} is the delamination length at

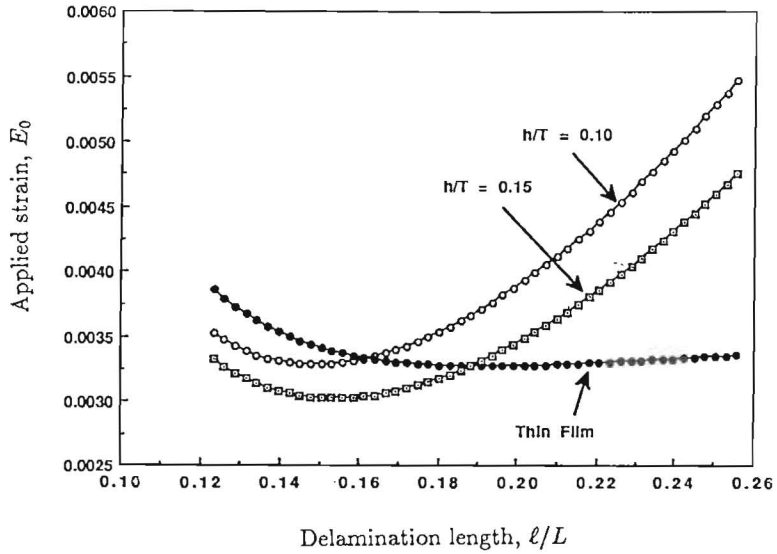

Fig. 5. The applied strain as a function of the delamination length (for a specific energy release rate $(2\Gamma/Eh)10^5 = 1.3$). In these curves, the lowest value (zero slope) is the unstable-to-stable transition point.

Table 1. $E_0/\varepsilon_{cr}(\ell_{tr})$ at the unstable-to-stable growth transition point*

	From the $G-\ell$ curves, E_0 is the applied strain		
	$h/T = 0.15$	$h/T = 0.10$	Thin film
$E_0 = 2.8 \times 10^{-3}$	1.82	1.86	3.00
$E_0 = 3.0 \times 10^{-3}$	1.81	1.85	3.00
	From the $E_0-\ell$ curves, $\tilde{\Gamma}_0 = (2\Gamma_0/Eh)10^5$, where Γ_0 is the critical energy release rate		
	$h/T = 0.15$	$h/T = 0.10$	Thin film
$\tilde{\Gamma}_0 = 1.0$	1.85	1.87	3.00
$\tilde{\Gamma}_0 = 1.3$	1.83	1.85	3.00

* Mode-independent fracture criterion, $\lambda = 1.0$

this transition point) for the general case is less than three.

A comparison of the ratio $E_0/\varepsilon_{cr}(\ell_{tr})$ for the cases examined is shown in Table 1. It is also seen that this ratio shows in general a tendency to increase for a smaller value of the ratio h/T (i.e. delaminations located closer to the surface).

Figure 6 illustrates the effect of varying the applied strain E_0 in the $G-\ell$ curves by showing a family of curves for $h/T = 0.15$ and the thin film solution for two values of applied strain. Although the ratio $E_0/\varepsilon_{cr}(\ell_{tr})$ is independent of the applied strain in the thin film solution, it is found that in the general case this ratio does have a slight dependence on the applied strain E_0 (see also Table 1).

The last two plots show the effect of mode dependence on the fracture criterion. For these plots, the energy release rate is normalized with the (mode-dependent) critical energy release

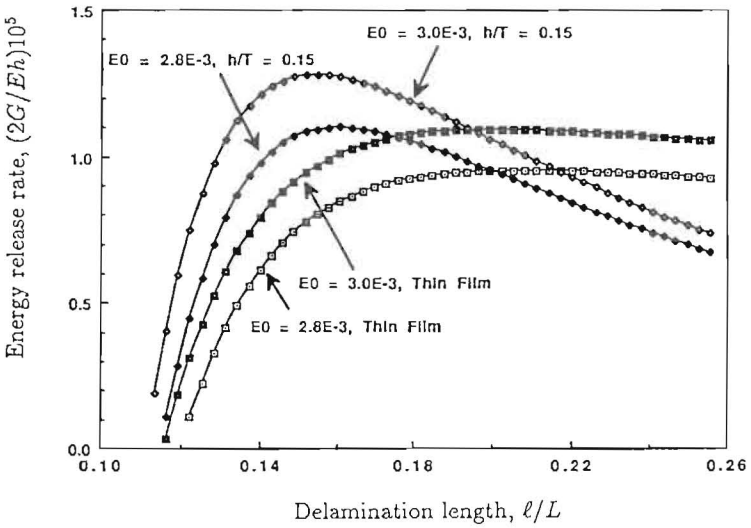

Fig. 6. The effect of applied strain on the growth stability (two values of E_0 are shown).

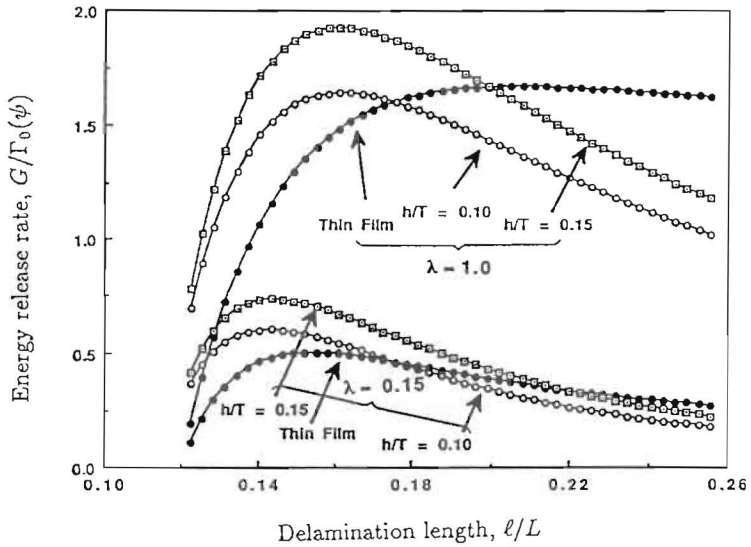

Fig. 7. The effect of mode-dependence on the fracture criterion ($\lambda = 1$ corresponds to mode-independence). An applied strain $E_0 = 2.8 \times 10^{-3}$ has been assumed.

rate $\Gamma_0(\psi)$. For this purpose, a value of $G_{IC} = 80\,\text{N/m}$ was assumed. Figure 7 gives the $G - \ell$ curves for an applied strain $E_0 = 2.8 \times 10^{-3}$ for two values of λ : $\lambda = 1$ corresponding to mode-independence, and $\lambda = 0.15$ according to the mode-dependent fracture criterion (28). Again, the cases of $h/T = 0.10$, 0.15 and the thin film solution are shown. It is seen that the unstable-to-stable transition point in the $\lambda = 0.15$ case is shifted to the left (smaller delamination lengths) in comparison to the mode-independent $\lambda = 1.0$ curves. For the $h/T = 0.10$, 0.15 cases, the ratio $E_0/\varepsilon_{cr}(\ell_{tr})$ is reduced to about 1.5 versus 1.8 for the $\lambda = 1$ case. For the thin film model this ratio is reduced to 1.7 for $\lambda = 0.15$ versus the value of three for $\lambda = 1$.

Furthermore, the values of the ratio $G/\Gamma_0(\psi)$, which determines whether growth takes place, show a wide range, increasing to above unity for the $\lambda = 1$ curves but remaining

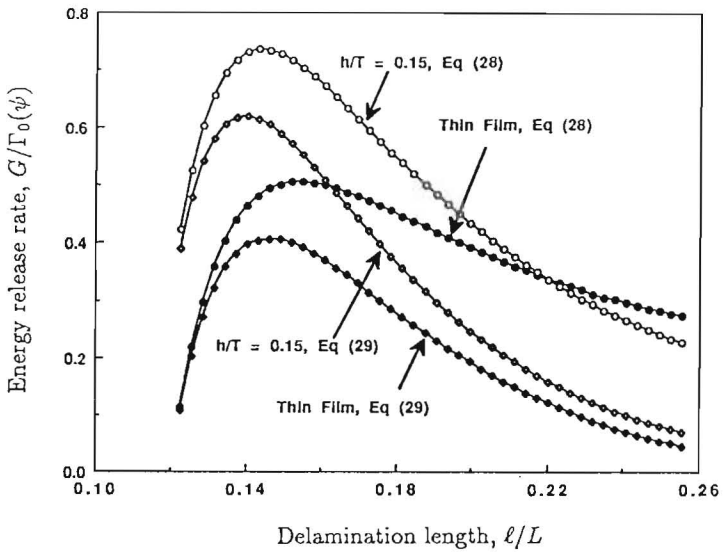

Fig. 8. Comparing the predictions of the two suggested mode-dependent fracture criteria for an applied strain $E_0 = 2.8 \times 10^{-3}$.

below unity for the $\lambda = 0.15$ curves (and being always higher for the larger values of h/T). This underlines the importance of the combined influence of the relative location of the delamination through the thickness, and that of the selection of the appropriate fracture criterion. The latter is also underscored in Fig. 8 which compares the predictions of the two suggested fracture criteria, (28) and (29) for $\lambda = 0.15$ (again for $h/T = 0.15$ and the thin film solution, and for an applied strain $E_0 = 2.8 \times 10^{-3}$). It is seen that the unstable-to-stable transition point for the fracture criterion (29), is shifted slightly to the left in comparison to employing the fracture criterion (28) with the same λ. For the $h/T = 0.10$, 0.15 cases, the ratio $E_0/\varepsilon_{cr}(\ell_{tr})$ was calculated to about 1.4 versus 1.5 for the (28) case. For the thin film model this ratio is reduced to 1.5 for (29) versus the value of 1.7 for (28).

Before listing these results in a condensed form, it is useful to re-iterate the major outcome of this research. In short, besides providing a formulation and solution for investigating the stability of delamination growth for an arbitrary ratio h/T of the relative delamination thickness, this work shows clearly that delamination growth is more likely to be stable than would be expected on the basis of the thin film model.

This study is a one-dimensional analysis and it is, therefore, natural to underline the need that the stability of growth be studied in detail in the future for two- dimensional delamination configurations. To this extent, Nilsson and Storåkers [18] have found in their numerical study of a single embedded circular delamination under uniaxial compression that the external load required to sustain crack growth for their configuration was steadily decreasing, rendering the system unstable, and this result was sensitive to the particular fracture criterion used. Further studies are needed to study the stability of delamination growth in the more common, two-dimensional, elliptical delaminations.

6. Conclusions

In this study, the closed form solutions for the energy release rate at the delamination tip versus applied compressive strain during the initial postbuckling phase were used to define

the combinations of delamination length and applied strain that lead to unstable growth. This would practically cause a 'jump' (most probably contained) growth of the delamination. Specifically, the following were concluded from this investigation:

1. Thin film theory predicts that at the transition point of unstable to stable growth ℓ_{tr} the ratio of the applied strain and the critical delamination buckling strain $\varepsilon_0/\varepsilon_{cr}(\ell_{tr})$ is three; the present study predicts that for an increasing value of the relative delamination thickness h/T the ratio $\varepsilon_0/\varepsilon_{cr}(\ell_{tr})$ is less than three, and is dependent on the fracture toughness. This indicates that the point of stable growth is occurring at a smaller delamination length (than the thin film model).
2. Another observation is that beyond the transition point (peak point in the $G - \ell$ curves), the curves for an increasing h/T ratio are steeper than the thin film model approximation; therefore, the jump distance when unstable growth occurs, is smaller than the one predicted by the thin model.
3. A study of the influence of the mode dependence of interface toughness on the conditions of initiation and extent of delamination growth reveals that the unstable-to-stable transition point in the mode-dependent cases is shifted to the left (smaller delamination lengths) in comparison to the mode-independent curves, and the ratio $\varepsilon_0/\varepsilon_{cr}(\ell_{tr})$ is accordingly decreasing.
4. A common, major observation from the results of this work is that delamination growth is more likely to be stable than would be expected on the basis of the thin film model.

Acknowledgement

The financial support of the Office of Naval Research, Mechanics Division, Grant N00014-91-J-1892, and the interest and encouragement of the Grant Monitor, Dr. Y. Rajapakse, are both gratefully acknowledged.

References

1. W. Johnson and S.K. Ghosh, *Journal of Materials Science* 16 (1981) 285–301.
2. H. Chai, C.D. Babcock and W.G. Knauss, *International Journal of Solids and Structures* 17 (1981) 1069–1083.
3. G.A. Kardomateas and D.W. Schmueser, *AIAA Journal* 26 (1988) 337–343.
4. V.V. Bolotin, *Mechanics of Composite Materials (Mekhanika Kompozitnykh Materialov* 3 (1987) 424–432.
5. G.A. Kardomateas, *AIAA Journal* 27 (1989) 624–631.
6. S.S. Wang, N.M. Zahlan and H. Suemasu, *Journal of Composite Materials* 19 (1985) 296–316.
7. G.J. Simitses, S. Sallam and W.L. Yin, *AIAA Journal* 23 (1985) 1437–1444.
8. H Chai and C.D. Babcock, *Journal of Composite Materials* 19 (1985) 67–97.
9. W.-L. Yin, *Proceedings, 27th SDM AIAA/ASME/ASCE/AHS Conference*, Paper 86-0883, San Antonio, Texas (1986) 165–179.
10. B. Storåkers and B. Andersson, *Journal of the Mechanics and Physics of Solids* 36 (1988) 689–718.
11. G.A. Kardomateas, *Journal of Applied Mechanics* (ASME) 60 (1993) 903–910.
12. Z. Suo and J.W. Hutchinson, *International Journal of Fracture* 43 (1990) 1–18.
13. S.J. Britvek, *The Stability of Elastic Systems*, Pergamon, New York (1973).
14. J.W. Hutchinson and Z. Suo, in *Advances in Applied Mechanics*, Vol. 29, Academic Press (1992) 63–191.
15. J. Dundurs, *Mathematical Theory of Dislocations*, American Society of Mechanical Engineers, New York (1969) 70–115.
16. A.J. Kinloch, *Adhesion and Adhesives*, Chapman and Hall, London (1987).
17. A.G. Evans and J.W. Hutchinson, *Acta Metallurgica et Materialia* 37 (1989) 909–916.
18. K.-F. Nilsson and B. Storåkers, *Journal of Applied Mechanics* (ASME) 59 (1992) 530–538.